Uncertainty and Sensitivity Analysis of Building Integrated Photovoltaics

Chen, L.[1], Tian, W. [1*], de Wilde, P.[2], Zhang, H.[1]
[1]College of Mechanical Engineering, Tianjin University for Science and Technology, China
[2]Department of Architecture, University of Strathclyde, United Kingdom
weitian@tust.edu.cn

Abstract. The performance of building-integrated photovoltaics (BIPV) shows high variations due to several factors, including design model uncertainty, installation mode, dirt/soil effects, aging factors, and manufacturing issues. This paper explores the uncertainty of BIPV outputs from the perspectives of both model uncertainty and parameter uncertainty using the EnergyPlus program. The sampling-based Monte Carlo method is implemented to conduct the uncertainty analysis of BIPV outputs. The meta-model global sensitivity analysis (Bayesian adaptive spline surfaces) is used to obtain important factors affecting BIPV outputs due to its high computational efficiency. The results indicate that both model and parameter uncertainty has significant influences on PV outputs. The combined remaining effect, power rating, and model uncertainty are three important factors influencing PV electricity. Therefore, these factors should be carefully chosen or adjusted to provide a reliable estimation of PV outputs.

1. Introduction

BIPV (building-integrated photovoltaics) has been widely considered a promising method to provide sustainable energy for buildings (Sun et al, 2021). There are different types of integration methods in buildings, including walls, roofs, windows, and skylights. Chen et al. (2021) investigate the energy performance of BIPV windows in street canyons. They found that energy savings due to BIPV window increase in north-south orientated open canyons. Pabasara et al. (2022) investigate the design options of building-integrated photovoltaics using multi-objective optimization in terms of life-cycle cost and energy performance. The method proposed includes four steps: data inputs, performance simulation, optimizer, and optimized results. The results show that there are seven optimum roof BIPV design solutions and fourteen skylight BIPV design options. Rounis et al. (2021) explore the design, development, and experiments of BIPV/T (building-integrated photovoltaics/thermal) in an indoor solar simulator. Their study provides a design standardization of air-based BIPV/T design and emphasizes the importance of convective heat transfer in this BIPV/T system. Most previous studies concentrate on the electricity and thermal performance of BIPV systems. There are studies to explore the uncertainty of PV systems. Liu et al. (2018) apply a two-stage procedure to predict both the point and interval estimation of short-term PV outputs. The first step is to create neural network models and the second step is to apply the kernel non-parameter density estimation to estimate the associated prediction intervals. Thenevard et al. (2013) discuss the long-term uncertainty of PV outputs. They found that the standard deviation of PV outputs is approximately 8.7% for the first year of operation and 7.9% for the other years over the PV lifetime. However, a few studies focus on both uncertainty and sensitivity analysis of building-integrated photovoltaics. The variations of energy performance in BIPV due to uncertain inputs are not fully explored yet.

Therefore, this research investigates the uncertain results of BIPV outputs and identifies the key factors affecting PV electricity. Both the model and parameter uncertainty in a BIPV system would be explored in this research. The meta-modeling sensitivity analysis is used to

https://doi.org/10.7146/aul.455.c196

obtain the sensitivity index influencing BIPV outputs. Moreover, the convergence of both uncertainty and sensitivity results for the BIPV system is evaluated to obtain robust results.

2. Method

The procedures of uncertainty and sensitivity analysis of building-integrated photovoltaics can be divided into six steps as illustrated in Figure 1. The first step is to determine the distributions of input parameters from previous studies. The second step is to obtain the sampling results using the Latin hypercube method. The third step is to compute the PV models with the EnergyPlus program in the R environment. The fourth step is to collect the PV electricity from the EnergyPlus models. The fifth step is to display the uncertain results of PV systems. The sixth step is to conduct the sensitivity analysis based on the meta-model global sensitivity analysis. The BP Solar BP275 PV panels are used in this case study. The area of a PV panel is 0.63 m^2 with 36 solar cells. The short-circuit current is 4.75 A and the open-circuit voltage is 21.4 V. More detailed information on these PV panels is available in the EnergyPlus example file (DOE, 2021).

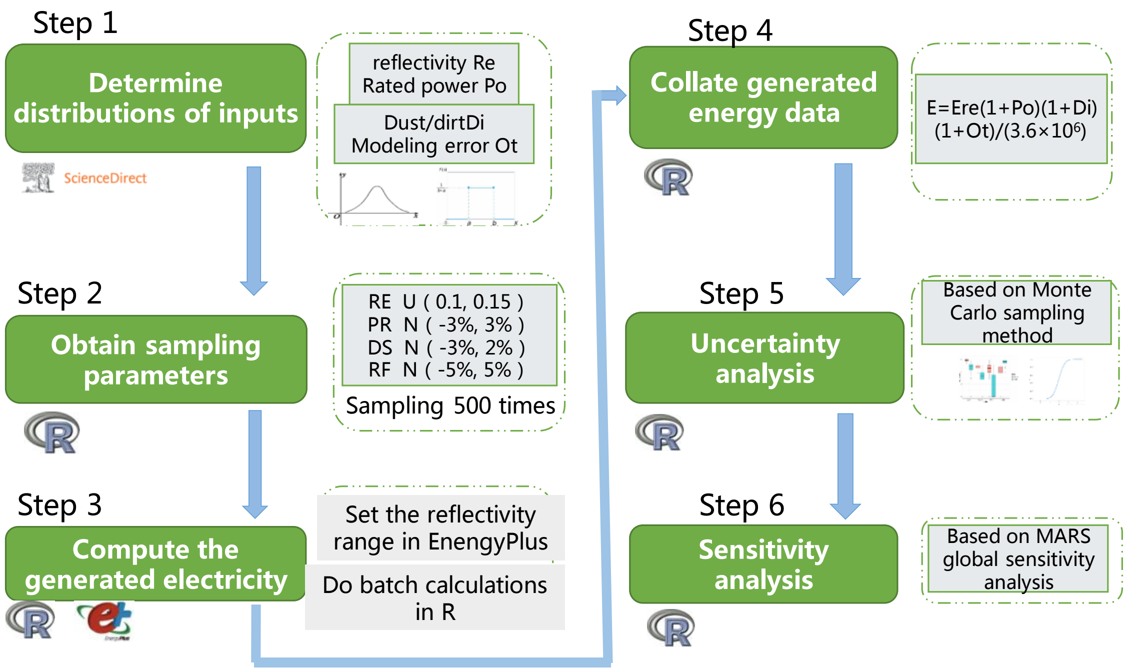

Figure 1: Flow chart of uncertainty and sensitivity analysis of building-integrated photovoltaics.

2.1 Uncertainty analysis

Two types of uncertainty will be considered in this study: model and parameter (Tian et al., 2018), as listed in Table 1. Model uncertainty refers to various PV models to estimate the electricity of PV systems, whereas parameter uncertainty refers to the parameters influencing PV outputs. Three types of PV models are considered: simple, TRNSYS, and Sandia (DOE, 2021). The simple PV model is used to compute the electricity output by the incident solar radiation multiplying the constant PV efficiency. The TRNSYS model is a four-parameter empirical equivalent circuit model to estimate the PV output (Duffie and Beckman, 2013). The Sandia model is developed by David King from the Sandia National Lab using empirical relationships (King et al., 2003). The uncertain parameters include installation modes, Albedo, power rating, dirt/soil, and other variables. Two types of installation modes are considered: stand-alone (decoupled) and natural ventilation, which can be regarded as a uniform categorical variable. For standalone PV, the cell temperature of modules in the array is obtained from the energy balance relative to NOCT (Nominal operating cell temperature) conditions. The NOCT temperature is the operating temperature of the module with a wind speed of 1 m/s, no electrical load, and a certain specified insolation (800 W/m2) and 20oC ambient temperature (Beckman and Duffie, 2013). For the natural ventilation BIPV, the PV temperature is obtained from the exterior baffle temperature in the naturally ventilated exterior cavity model. The albedo is taken as a uniform distribution between 0.1 and 0.15. The change of PV power rating is regarded as a normal distribution of mean -3% and standard deviation of 3%. The influence of soil and dirt is represented as a normal distribution of mean -3% and a standard deviation of 2%. The remaining variables including spectral effects, aging effects, etc. (named as other variables) are considered as a normal distribution of a mean of -5% and a standard deviation of 5% (Thevenard and Pelland, 2013).

Table 1: Uncertainty parameters for uncertainty and sensitivity analysis of PV system.

Uncertainty type	**Factor**	**Short names**	**Values/Distributions**
Model uncertainty	PV computation method	PM	Simple (SP), TRNSYS (TS), Sandia (SN)
Parameter uncertainty	Installation mode	IM	Stand-alone (DE), natural ventilation (VN)
	Albedo	RE	U(0.1, 0.15)
	Power rating	PR	N(-3%, 3%)
	Dirt soil	DS	N(-3%, 2%)
	Remaining factors	RF	N(-5%, 5%)

The PV panel is assumed to be installed in Tianjin, China, and the typical year data in Tianjin is used to obtain PV electricity. Figure 2 shows the variations of daily solar radiation in different months. There are more variations of daily solar radiation in summer than those in winter. The simulation is conducted using the EnergyPlus V9.6 program (DOE, 2021). There are three types of PV models and two types of installation modes. Hence, there are 6 cases in this study. The PV models are run 1000 times using the Sobol sampling method to obtain reliable results of PV outputs for every case. The Sobol sequence is a low discrepancy quasirandom sequence with a good convergence performance (Sun, 2021). The convergence test of uncertainty and sensitivity analysis would be discussed in section 3.1 and section 3.2, respectively.

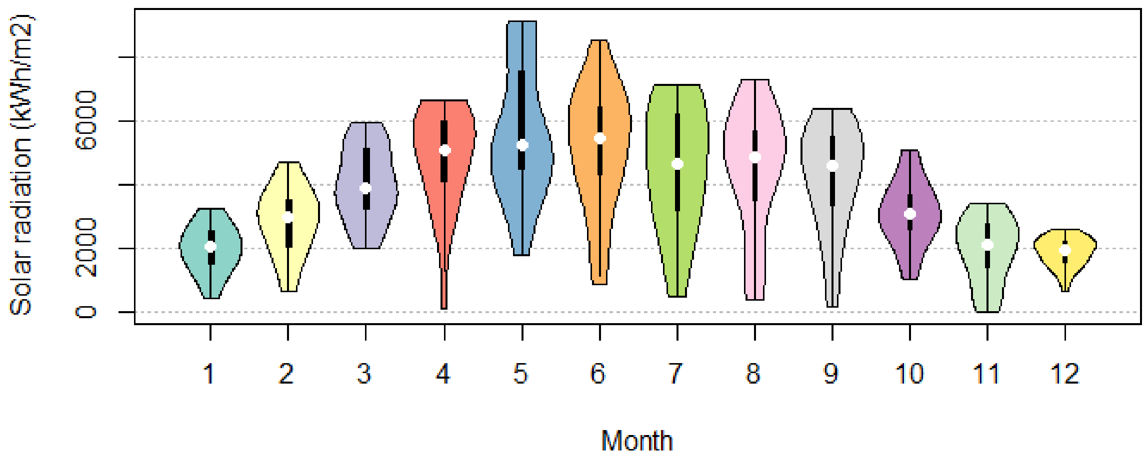

Figure 2: Violin plots for daily horizontal solar radiation by month in Tianjin.

2.2 Sensitivity analysis

The meta-modeling Sobol sensitivity analysis is conducted to obtain the importance rankings of the factors above influencing PV output (Tian, 2013). The meta-model used in this method (Bayesian adaptive spline surfaces) is one of the polynomial spline models in which the integrals can be computed analytically without the Monte Carlo simulation (Francom and Sanso, 2020). Hence, the computational efficiency would increase significantly compared to the conventional meta-model variance-based global sensitivity analysis. The Bayesian adaptive spline surface models are firstly created using the 1000 samples from the uncertainty analysis. Then the sensitivity index is derived based on the definition of the main and total effects of global sensitivity analysis. The main effects and total effects can be obtained at the same time from this meta-model sensitivity analysis. The main effects refer to the influences of a single factor without considering the effects of other factors, whereas the total effects include the main effects of one specific factor and interaction effects with the other factors. The interaction effects can be two-way or higher-order effects for a complex engineering system. R Bass package is used for sensitivity analysis (Francom and Sanso, 2020).

3. Results and discussion

3.1 Results from uncertainty analysis

This section would firstly discuss the convergence of uncertainty analysis of PV electricity to make sure the results are stable. Then the total uncertainty results would be described to compare the results in three PV computation methods and two installation modes. Finally, the uncertainty results would be illustrated due to separate factors.

Convergence of results from uncertainty analysis

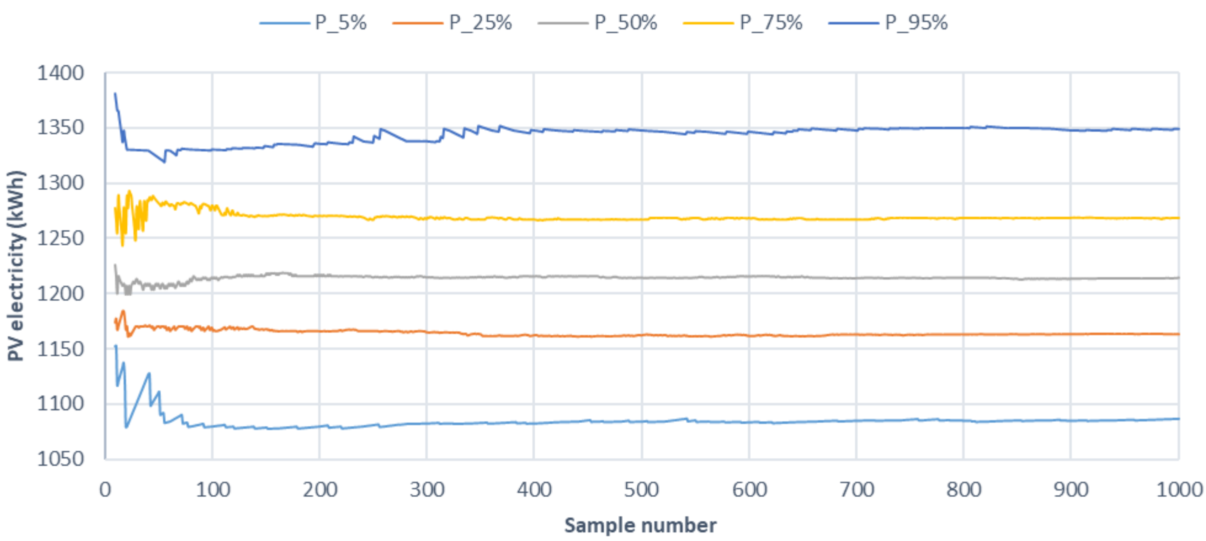

Figure 3: Stability of percentiles of electricity generated by PV systems with the sample number for the ventilation mode using the TRNSYS model.

It is necessary to check the convergence of uncertainty results using sampling-based methods. Figure 3 shows the change of various percentiles of PV electricity with the ventilation mode using the TRNSYS model. These percentiles tend to be stable after 400 simulation runs using the Sobol sequence sampling method. The 95th percentile of PV electricity has more variations in this case study as might be expected. This is because more extreme values require more sampling runs. The 50th percentile (median) of PV electricity has slight variations after 200 simulation runs. The 1000 sample runs are chosen in this research for the stable results of both uncertainty and sensitivity analysis. The convergence of sensitivity results would be discussed in section 3.2.

Results from total uncertainty analysis Figure 2 and Figure 3 show the cumulative density function and box plots of annual electricity in six cases, respectively. The model uncertainty has a marked influence on the results of PV electricity. The results from the simple model (SP) are almost the same for two installation modes (stand-alone and natural ventilation), whereas the results from the stand-alone are around 12% higher than those from the natural ventilation using the Sandia model and TRNSYS model. This is because the influences of change in PV temperature can be properly considered in the more detailed PV models, including Sandia and TRNSYS models. Hence, it is necessary to implement suitable PV models in estimating PV outputs when integrating with buildings. As also can be seen from Figure 3, the differences in mean values from the Sandia and TRNSYS models are less than 2%. As a result, the PV electricity using both the Sandia and TRNSYS is reliable to provide an accurate estimation of PV outputs.

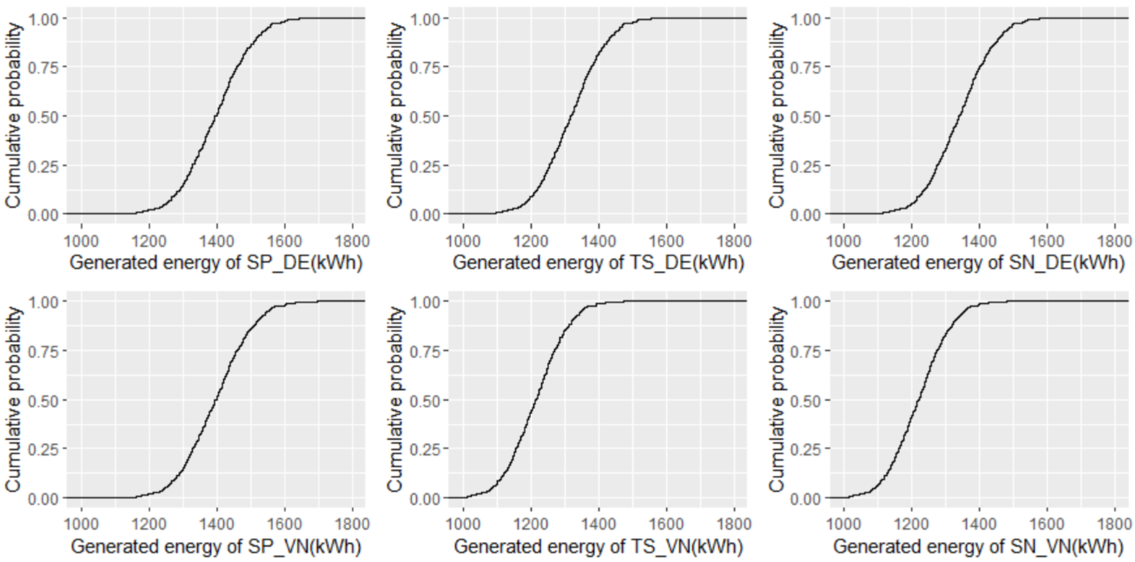

Figure 4: Electricity generated by PV systems in two installation modes (DE, decoupled; VN, ventilation) and three PV models (SP, simple; TS, TRNSYS; SN: Sandia National Laboratories).

The IQR (inter-quartile range) values of PV electricity are 132 kWh when using the simple PV model. These IQR values would be decreased to 124 kWh in the case of stand-alone PV installation mode using the TRNSYS and Sandia models. The IQR values would further slightly be reduced in the case of natural ventilation BIPV. Hence, the uncertainty of PV electricity would change with the variations of PV models and PV installation modes although the change of uncertainty is not significant. It is also found that the coefficients of variation for PV outputs in all six cases are around 6.44% in this research. This suggests that the relative variations of PV electricity normalized to the mean values for three PV computation methods and two installation modes are almost the same in this case study. As also can be seen from Figure 5, the ranges of PV outputs in every case study are larger than the difference between the three PV computation methods. Hence, the variations of PV electricity due to the parameter uncertainty are larger than those from the model uncertainty.

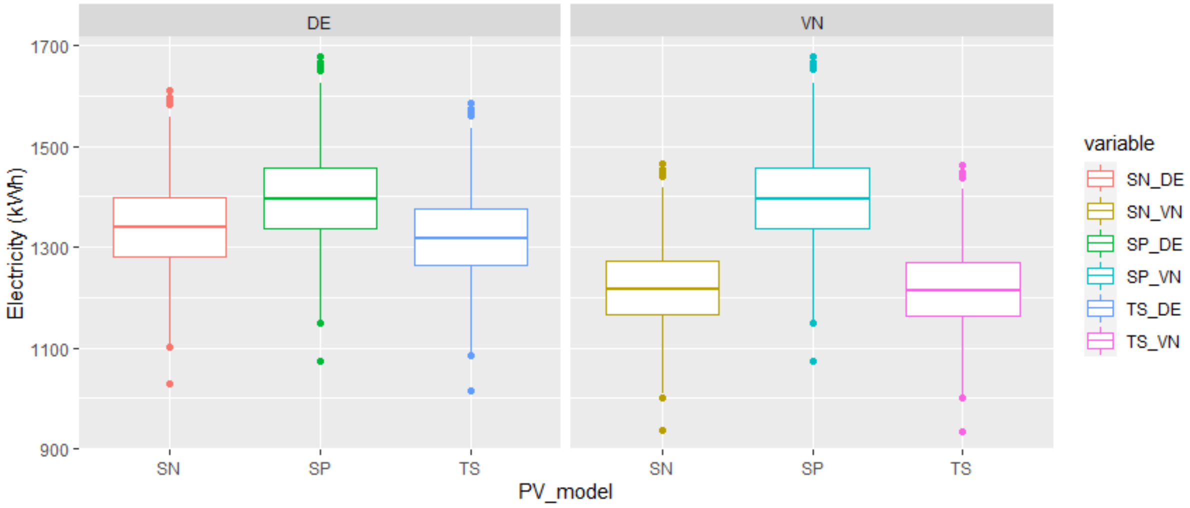

Figure 5: Box plots of electricity generated by PV systems in two installation modes (DE, decoupled; VN, ventilation) and three PV models (SP, simple; TS, TRNSYS; SN: Sandia National Laboratories).

Results from uncertainty analysis from four separate factors It is also interesting to explore the density plots for separate factors in a specific PV computation method and a specific installation mode. The PV electricity with the ventilation mode and TRNSYS method would be investigated because this PV calculation method can present more reliable results as discussed in this section. Figure 6 illustrates the kernel density plots of PV electricity due to four factors: Albedo (RE), power rating (PR), dirt/soil (DS), and other variables (RF). The largest variation of PV electricity is due to the RF (other variables, including aging and spectral effects) in which the interquartile is 92 kWh. The next factor is PR (power rating) with the interquartile of 55 kWh. The third-largest variation of PV electricity is because of dirt on the PV surface and its variation only accounts for around one-third of variations due to RF factors. There are almost no variations of PV electricity due to RE (Albedo) in this case study.

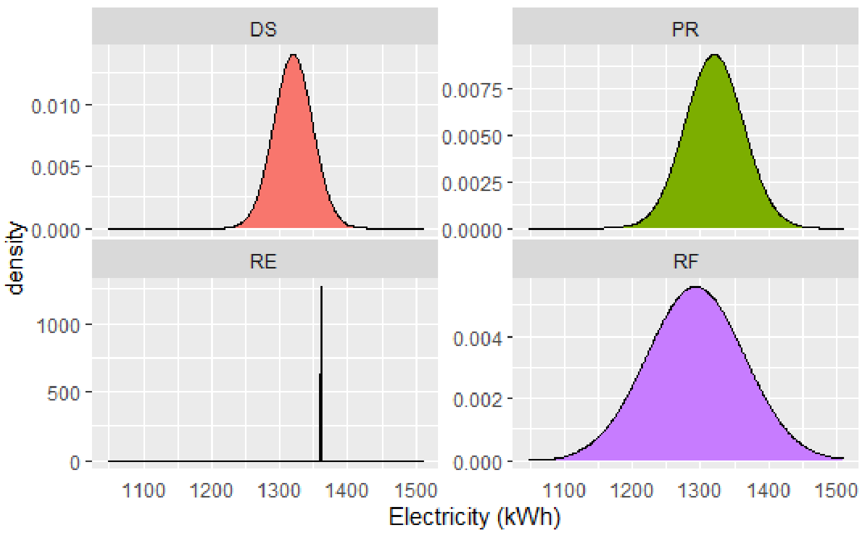

Figure 6: Density plots of PV electricity using the TRNSYS model in the ventilation mode due to four factors (DS, dirt soil; PR, power rating; RE: reflectivity; RF, remaining factors).

3.2 Results from sensitivity analysis

This section firstly presents the convergence of the sensitivity index with the sample size. Then the main effects and interactions influencing PV electricity are illustrated. Finally, the total effects would be explored to obtain the final importance rankings affecting PV outputs in this case study.

Convergence of results from sensitivity analysis Figure 6 shows the change of total effects as a function of sample size in this case study. The total effects obtained from sensitivity analysis would be very unstable before the 300 simulation runs. The ranking results for PM (PC computation method) and PR (power rating) would be even changed after 100 simulation runs. After the 500 simulation models, the total effects become stable although there exists a slight change after 900 model runs. The simulation runs for stables results between uncertainty and sensitivity analysis are different by comparing Figure 4 and Figure 6. In this case study, more simulation runs are required for sensitivity analysis than those for uncertainty analysis.

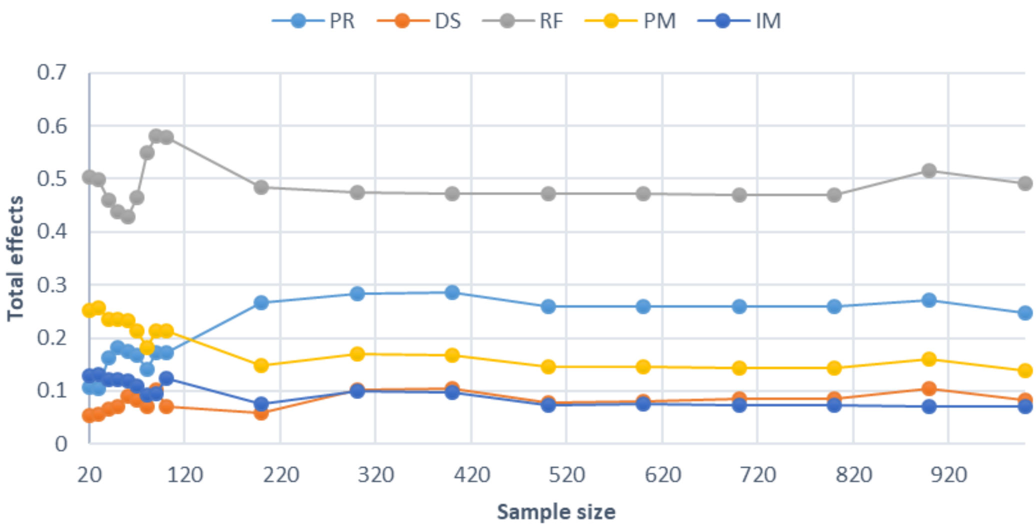

Figure 6: Stability of total effects with the sample number for the PV systems.

Main effects and two-way interactions

Figure 7 shows the sensitivity results of input parameters using the meta-model global sensitivity analysis. The most important factor is the remaining variables, including spectral effects, aging effects, etc., which account for around 58% of variations of PV outputs. The next two important factors are the PV power rating and model uncertainty, which are responsible for 17% and 11% of output variations, respectively. The sum of these three important factors accounts for approximately 86% of total variations of PV outputs. The other factors have only slight influences on the variations of PV outputs. Hence, these three factors should be carefully considered in computing PV outputs to properly evaluate the uncertainty of electricity generated from the BIPV system. As also can be seen from Figure 4, the interactions of the PV model and installation modes also have influenced the variations of PV outputs. This can be explained from Figure 3 that the PV results would be changed in two installation modes using the Sandia or TRNSYS models, while the PV outputs would almost be the same in two different installation modes using the simple PV model.

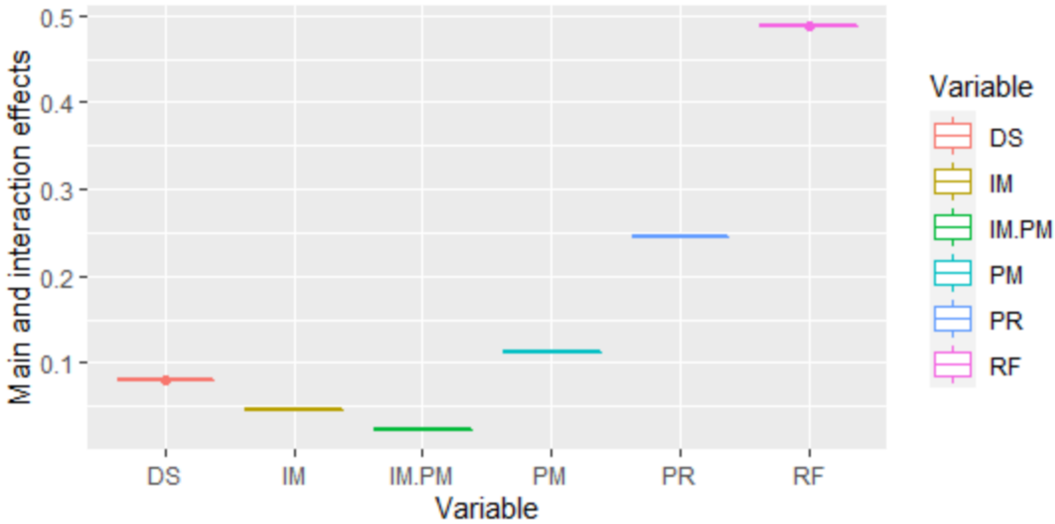

Figure 7: Main and interaction effects of input parameters influencing PV electricity.

Total effects

Figure 8 shows the total effects of factors influencing PV electricity. A similar conclusion can be obtained as discussed in Figure 7. The total effects are almost the same as the main effects for three factors, including RF, PR, and DS, since there are almost no interactions between these three factors. The total effects for both IM and PM would be increased by around 0.0234 due to the interactions of these two factors as shown in Figure 7. Therefore, the total sensitivity index for all the factors would be above one due to the interactions. It can be also observed that the variations of total effects are very small in this case. Therefore, the rankings results influencing PV electricity would be very robust since there are no overlapping total effects. The albedo effects have almost no influence on PV outputs in this case study, which are not shown in Figure 8. The RF (including aging, spectral, and other variables) has a large influence on the PV outputs. More detailed research is required to decompose this combined factor into specific variables, which could provide more guidance on how to reduce the uncertainty of PV estimation.

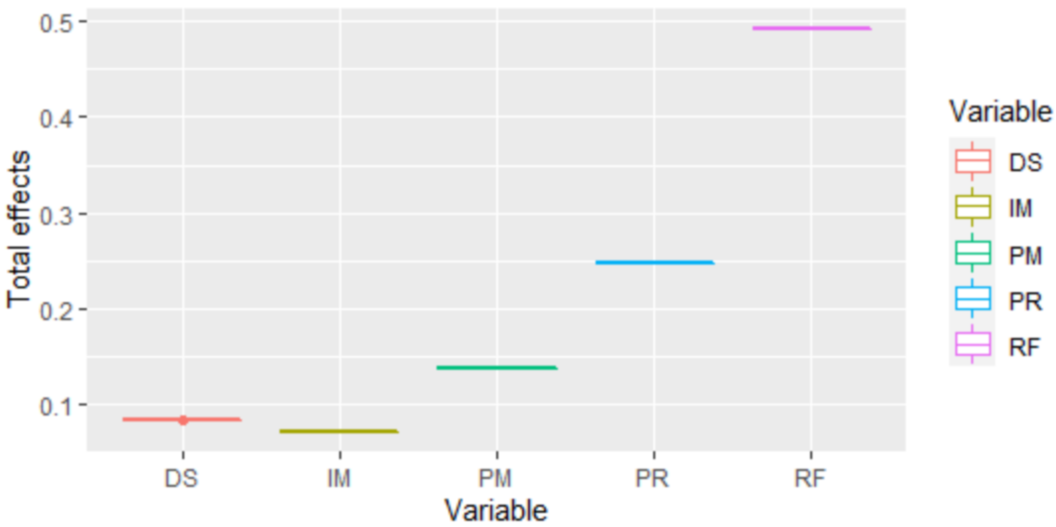

Figure 8: Total effects of input parameters influencing PV electricity.

4. Conclusion

This paper investigates the uncertainty and sensitivity analysis of building-integrated photovoltaics (BIPV) from the perspective of both model and parameter uncertainty. The following conclusions have been obtained from this research:

(1) The convergence of uncertainty and sensitivity in exploring the BIPV performance should be properly evaluated. In this case study, more simulation runs for the sensitivity analysis are required compared to the uncertainty analysis.

(2) The results from uncertainty analysis indicates that both model and parameter uncertainty have significant influences on PV outputs. The variations of PV electricity due to the parameter uncertainty are larger than those due to the model uncertainty.

(3) The results from the meta-model sensitivity analysis show that the remaining effects (including aging and spectral effects), power rating, and model uncertainty are three important factors influencing PV electricity. Therefore, these factors should be carefully chosen or adjusted to provide a reliable estimation of PV outputs.

Further research is be required to understand the effects of uncertain factors for different types of BIPV, such as PV windows, and PV/T systems.

Acknowledgments

This research was supported by the National Natural Science Foundation of China (No. 51778416) and the Key Projects of Philosophy and Social Sciences Research, Ministry of Education (China) “Research on Green Design in Sustainable Development” (contract No. 16JZDH014).

References

Chen L., Zheng X., Yang JC., Yoon JH., (2021) Impact of BIPV windows on building energy consumption in street canyons: Model development and validation, Energy and Buildings, 249, 111207

DOE (2021) EnergyPlus V9.6 September 2021, Department of Energy, USA.

Duffie, John A., and William A. Beckman. 2013. Solar Engineering of Thermal Processes. New

York: John Wiley & Son

Francom, D., Sanso, B. (2020). BASS: An R Package for Fitting and Performing Sensitivity Analysis of Bayesian Adaptive Spline Surfaces. Journal of Statistical Software, **94**(8), pp. 1–36.

King, D.L., Boyson, W.E., Kratochvil J.A. 2003. Photovoltaic Array Performance Model. Sandia National Laboratories, Albuquerque, NM 87185, November 2003.

Liu, L., Y. Zhao, D. Chang, J. Xie, Z. Ma, Q. Sun, H. Yin and R. Wennersten (2018). "Prediction of short-term PV power output and uncertainty analysis." Applied Energy 228: 700-711.

Pabasara Upalakshi Wijeratne, W.M. Tharushi Imalka Samarasinghalage, Rebecca Jing Yang, Ron Wakefield, (2022). Multi-objective optimisation for building integrated photovoltaics (BIPV) roof projects in early design phase, Applied Energy, 309,118476.

Rounis, E.D., Athienitis, K. A., Stathopoulos T., (2021). BIPV/T curtain wall systems: Design, development and testing, Journal of Building Engineering, 42,103019.

Sun, H., Heng, C.K., Tay S.E.R, Chen T., Reindl T., (2021). Comprehensive feasibility assessment of building integrated photovoltaics (BIPV) on building surfaces in high-density urban environments, Solar Energy, 225, pp. 734-746.

Sun, X., B. Croke, S. Roberts, A. J. R. E. Jakeman and S. Safety (2021). "Comparing methods of randomizing Sobol′ sequences for improving uncertainty of metrics in variance-based global sensitivity estimation." 210: 107499.

Thevenard, D., Pelland, S. (2013). Estimating the uncertainty in long-term photovoltaic yield predictions,

Solar Energy, 91, pp. 432-455.

Tian, W., Heo, Y., de Wilde, P., Li, ZY, Yan, D., Park C.S., Feng, XH, Augenbroe, G. (2018) A review of uncertainty analysis in building energy assessment. Renewable and Sustainable Energy Reviews, 93, 285-301.

Tian, W. A review of sensitivity analysis methods in building energy analysis, Renewable and Sustainable Energy Reviews, 2013, 20, 411-419.